PHYSICAL REVIEW B **85**, 100407(R) (2012)

Block antiferromagnetism and checkerboard charge ordering in the alkali-doped iron selenides $R_{1-x}Fe_{2-y}Se_2$

Wei Li,[1] Shuai Dong,[2] Chen Fang,[3] and Jiangping Hu[3,4,*]

[1]*Department of Physics, Fudan University, Shanghai 200433, China*

[2]*Department of Physics, Southeast University, Nanjing 211189, China*

[3]*Department of Physics, Purdue University, West Lafayette, Indiana 47907, USA*

[4]*Beijing National Laboratory for Condensed Matter Physics, Institute of Physics, Chinese Acadmey of Sciences, Beijing 100080, China*

(Received 6 October 2011; revised manuscript received 14 February 2012; published 23 March 2012)

By performing first-principles electronic structure calculations and analyzing effective magnetic model of alkali-doped iron selenides, we show that the materials without iron vacancies should approach a checkerboard phase in which each of the four Fe sites group together in a tetragonal structure. The checkerboard phase is the ground state with a block antiferromagnetic (AFM) order and a small charge density wave order in the absence of superconductivity. Both of them can also coexist with superconductivity. The results can explain the 2×2 ordered patterns and hidden orders observed in various different experiments, clarify the missing link between AFM and superconducting phases, suggest that the block-AFM state is the parent state, and can unify the understanding of various observed phases in alkali-doped iron selenides.

DOI: 10.1103/PhysRevB.85.100407 PACS number(s): 74.70.Xa, 74.25.Jb, 74.25.Ha, 74.20.Mn

Alkali-doped iron selenide superconductors[1–3] have attracted much research attention because of several distinct characteristics that are noticeably absent in other iron-based superconductors, such as the absence of hole pockets at the Γ point of the Brillouin zone in their superconducting (SC) phases[4–6] and antiferromagnetic (AFM) ordered insulating phases[7–9] with very high Néel transition temperatures in their parental compounds.[3] Due to these distinct physical characteristics from their pnictide counterparts, $R_{1-x}Fe_{2-y}Se_2$ are expected to be ideal grounds to test theoretical models of iron-based superconductors. Models based on different mechanisms have suggested different pairing symmetries for $R_{1-x}Fe_{2-y}Se_2$: Weak-coupling approaches based on spin-excitation mediated pairing predict a d-wave pairing symmetry,[10–13] strong-coupling approaches[14–16] which emphasize the importance of next-nearest-neighbor (NNN) AFM local exchange coupling suggest that the pairing symmetry is a robust s wave, not different from the $S^{\pm}$-wave symmetry obtained in their pnictide counterparts, and models with orbital fluctuation mediated pairing suggest a S^{++}-wave pairing for both iron selenide and pnictide materials.[17]

While the iron selenide superconductors have generated considerable excitement, there is deep confusion regarding the delicate interplay between Fe vacancies, magnetism, and superconductivity. Many of the latest experimental results in $R_{1-x}Fe_{2-y}Se_2$ indicate that the insulating AFM and SC phases are phase separated.[18–24] In particular, recent scanning tunneling microscopy (STM) measurements on $K_{1-x}Fe_{2-y}Se_2$ clearly suggest phase separation.[21,22] The material was shown to be phase separated into iron-vacancy-ordered regions and iron-vacancy-free regions. The former is insulating and shows a $\sqrt{5} \times \sqrt{5}$ vacancy-ordered pattern while the latter is SC. The neutron-scattering experiments have shown that the $\sqrt{5} \times \sqrt{5}$ vacancy-ordered phase is also AFM ordered.[7] More surprisingly, the AFM order is affected by SC pairing,[8] a result that is difficult to be understood within the picture of phase separation. In addition to the $\sqrt{5} \times \sqrt{5}$ vacancy-ordered phase, an insulating phase with a 2×2 ordered pattern was also observed.[19,20,25] Moreover, in the SC state where there is little vacancy, both STM[21,22] and angle-resolved photoemission spectroscopy (ARPES) experiments[6] suggest that there is an additional symmetry-breaking order in the SC phases.[6,21,22] The microscopic origin of this order and how it is related to the AFM phase are not understood.

In this Rapid Communication, we show that alkali-doped iron selenide superconductors without iron vacancies should approach a checkerboard phase in which each of the four Fe sites group together in a tetragonal structure. This broken-symmetry state is essentially driven by the same magnetic exchange couplings that drive the insulating AFM phase in the $\sqrt{5} \times \sqrt{5}$ vacancy-ordered state. We perform first-principles electronic structure calculations and develop an effective magnetic model to show the existence of such a broken-symmetry state. The checkerboard phase is the ground state with a block-AFM (BAF) order in the absence of superconductivity. The BAF fluctuations and the checkerboard lattice distortion are strongly coupled. A weak BAF order and the checkerboard lattice distortion can coexist with superconductivity. These results essentially suggest the BAF-ordered state is the parent state of alkali-doped iron selenide superconductors. The results consistently explain the 2×2 ordered pattern, which was misunderstood as another vacancy-ordered state, and the STM and ARPES experimental results.[6,21] This study clarifies the missing link between AFM and SC phases and essentially unifies the understanding of various observed phases.[19]

We start with the following simple question: If the system is free of iron vacancies, what should be the ground state if it does not become SC? To answer this question, we perform a first-principles calculation to investigate the ground state of an iron-vacancy-free domain. The calculated crystal structure is shown in Fig. 1(a). We calculated the energy of a number of different possible magnetically ordered states, including nonmagnetic (NM), ferromagnetic (FM), collinear-AFM (CAF, the state observed in iron pnictides[26,27]), bicollinear-AFM (BCAF, the state observed in FeTe),[28–32] and BAF, whose pattern is shown in Fig. 1(b) where four Fe sites group to form a supercell

 ©2012 American Physical Society

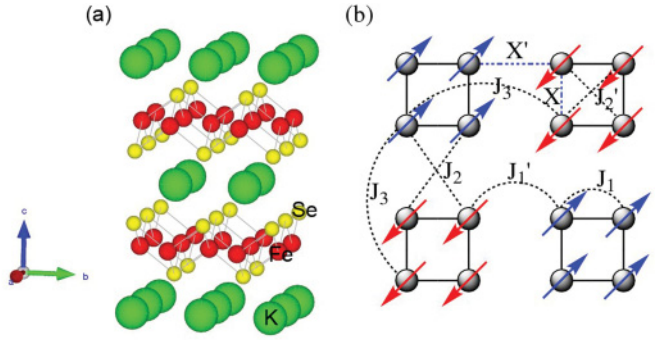

FIG. 1. (Color online) (a) The schematic crystal structure of KFe_2Se_2. The system consists of K (green, large), Fe (red, small dark), and Se (yellow, small light) atoms. (b) Schematic checkerboard lattice structure and spin ordering pattern in the BAF state. The lattice distortion is labeled by lattice constants X and X'. The magnetic exchange couplings are also indicated.

(note that in Ref. 33, BCAF is called E type and BAF is called X type). All these calculations were performed using the projected augmented-wave method[34] as implemented in the VASP code,[35] and the Perdew-Burke-Ernzerhof exchange correlation potential[36] was used. A 500-eV cutoff in the plane-wave expansion ensures the calculations converge to 10^{-5} eV. For each magnetic configuration, all atomic positions and the lattice constants were optimized until the largest force on each atom was 0.005 eV/Å. We used a $16 \times 16 \times 16$ Monkhorst-Pack k-grid Brillouin zone sampling throughout all of calculations.

The ground-state energies, the magnetically ordered moment, and their lattice constants in various states are listed in Table I. The BAF state clearly has the lowest energy in the optimized lattice tetragonal structure by using local density approximation (LDA) + U ($U = 2$ eV). Calculations with various U values show that our main results remain valid when U is varied for $U > 1$ eV. Without turning on U, our LDA results show that the ground state is BCAF, which is consistent with previous calculations.[33,37] In addition to the above results, the BAF state is also insulating with an energy gap of $E_g \approx 0.25$ eV.

From the standard symmetry analysis, since the BCAF state breaks the rotational symmetry of the lattice, it can couple strongly to a monoclinic lattice distortion. The BAF does not break the rotational symmetry of the lattice. Nevertheless, it can strongly couple to a lattice distortion pattern shown in Fig. 1(b). The lattice constant X (between two nearest sites in one supercell) and X' (between two supercells) as labeled in Fig. 1(b) are $X = 2.59$ Å, $X' = 3.04$ Å for $U = 2$ eV. This lattice distortion is comparable to the lattice distortion in the $\sqrt{5} \times \sqrt{5}$ vacancy-ordered $K_{0.8}Fe_{1.6}Se_2$ phase.[7] The lattice distortion quadruples the lattice unit cell to form a checkerboard pattern. In such a checkerboard lattice, charge ordering can take place. If we calculate the charge density difference (total density minus the sum of atomic densities) distribution around Fe atoms in the Fe layer, a charge ordering on the Fe layer is observed as shown in Fig. 2, which was observed in a recent STM experiment.[21] The fact that no monoclinic lattice distortion was observed in $R_{1-x}Fe_{2-y}Se_2$ experimentally also supports that the BAF state is the ground state in the absence of superconductivity.

TABLE I. Geometric, energetic, and magnetic properties of KFe_2Se_2 by using LDA + U ($U = 2.0$ eV) calculations. Results in the NM/FM/AFM/CAF/BCAF/BAF configurations using fully optimized structures are all shown. ΔE is the total energy difference per iron atom in reference to the optimized NM structure, and m_{Fe} is the local magnetic moment on Fe.

KFe_2Se_2	ΔE (eV/Fe)	a (Å)	b (Å)	c (Å)	$m_{Fe}(\mu_B)$
NM	0	3.8257	3.8257	13.3970	0
FM	−0.9931	4.0083	4.0083	14.4448	3.247
AFM	−0.7499	4.0824	4.0824	14.1749	2.959
CAF	−0.8304	3.9848	4.0625	14.3615	3.029
BCAF	−1.0639	3.9769	4.0482	14.2488	3.030
BAF	**−1.0957**	3.9824	3.9824	14.3882	3.056

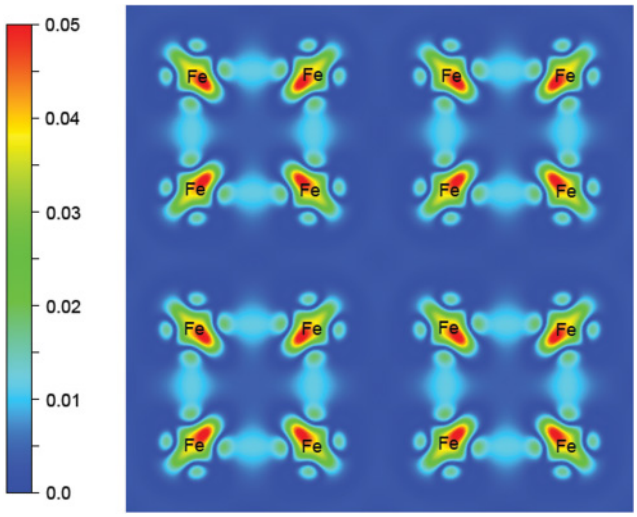

FIG. 2. (Color online) Charge density difference (total density minus the sum of atomic densities) distribution in the (001) plane crossing the first Fe atoms layer with a BAF-ordered state within the LDA + U ($U = 2$ eV) calculations.

Now we discuss the effective magnetic model that can interpret the above calculational results. It has been shown that a magnetic exchange J_1-J_2-J_3-K model,[38] where J_1, J_2, and J_3 are the nearest-neighbor (NN), NNN, and the next-NNN (NNNN) exchange couplings, respectively, and K is a spin biquadratic coupling term between two nearest-neighbor sites, is a good approximation to describe iron chalcogenides when the lattice distortion is ignored.[30,31,38,39] The calculated energies of the BCAF and BAF states in the unoptimized lattice tetragonal structure are almost degenerate. This degeneracy sows strong support for the model since these two states are exactly degenerate in the J_1-J_2-J_3-K classical spin model.[38] In the magnetically ordered state, the lattice distortion takes place and the tetragonal symmetry is broken. The NN exchange coupling J_1 can take two different values J_1 and J_1' as shown in Fig. 1(b). The biquadratic coupling K can be decoupled and treated as an effective difference between J_1 and J_1' as well.[38,40] In general, the NNN J_2 can also take two different values, J_2

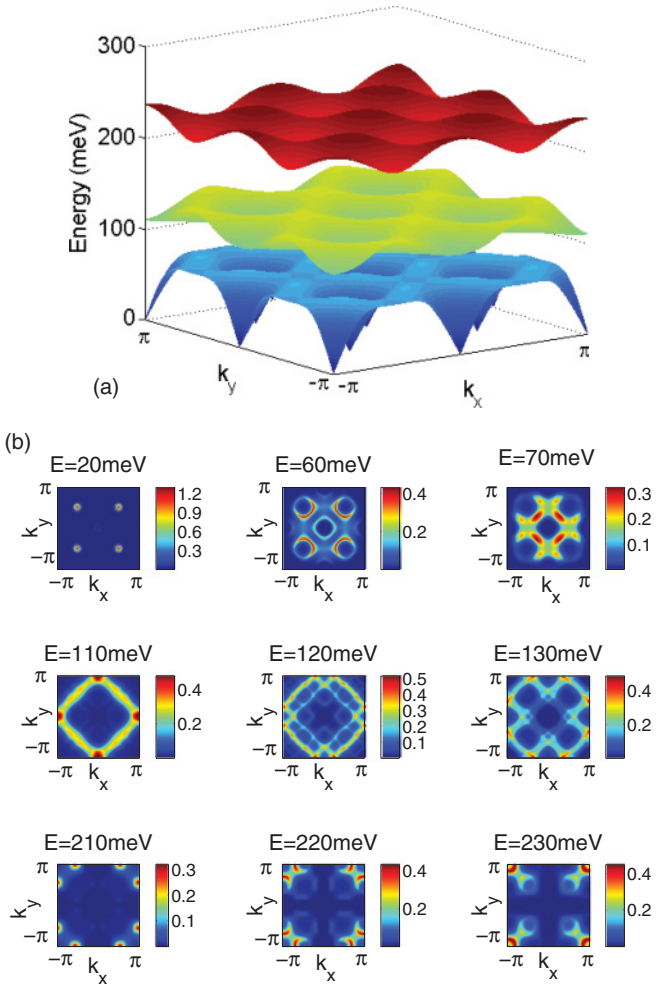

FIG. 3. (Color online) (a) Spin-wave dispersion and (b) imaginary part of dynamic susceptibility for the BAF state with the J_1-J_1'-J_2-J_3 model at $J_1 = -36$ meV, $J_1' = 15$ meV, $J_2 = 14$ meV, $J_3 = 9$ meV, taken from Ref. 9. The profile of the imaginary part of the dynamic susceptibility is plotted at various energies with an energy resolution of 5 meV, and it is given in arbitrary units.

and J_2', as also shown in Fig. 1(b). However, as has been proved in other iron-based superconductors, the NNN coupling J_2 is rather robust against lattice distortion. The difference between J_2 and J_2' is rather small. Therefore, the effective magnetic exchange model in the magnetically ordered state is given by J_1-J_1'-J_2-J_3, with J_1 being strongly FM and $J_{2,3}$ both being AFM. J_1' can be weak FM or weak AFM. A similar model has been shown to describe the magnetism of the $\sqrt{5} \times \sqrt{5}$ vacancy-ordered $K_{0.8}Fe_{1.6}Se_2$ phase.[9,39,41,42] Therefore, while the exact values of the magnetic exchange couplings cannot be accurately obtained from LDA calculations, since the lattice distortions in both cases are similar, it is reasonable to believe that these values should not be too different from those of $K_{0.8}Fe_{1.6}Se_2$, which has been measured by fitting neutron-scattering experiments.[9] The measured values, which are specified in Fig. 3, also give the BAF-ordered ground state. The energy saved from magnetic exchange coupling per site is given by $(-J_1 + 2J_3 + J_1')S^2$. This energy is slightly smaller than the magnetic energy saved in the vacancy-ordered

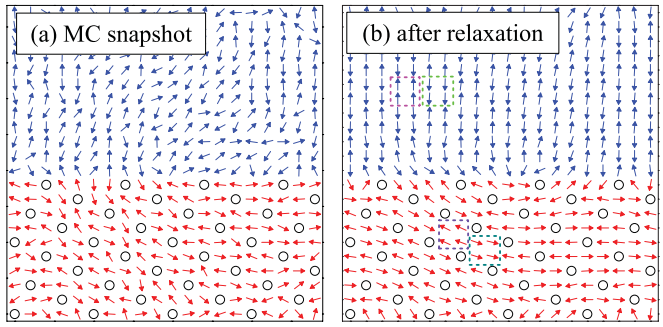

FIG. 4. (Color online) (a) A typical MC snapshot (after 3×10^4 MC steps) of the classical J_1-J_2-J_3-K magnetic model. (b) The spin pattern after the zero-T relaxation. In (a) and (b), spins in regions without vacancies (upper) and with vacancies (lower) are in blue (dark gray) and red (light gray), respectively. Black circles denote the vacancies.

$K_{0.8}Fe_{1.6}Se_2$.[9,39] The spin-wave dispersion and the imaginary part of the dynamic spin susceptibility of the BAF phase are shown in Fig. 3.

There is another interesting prediction if the same magnetic model describes both $K_{0.8}Fe_{1.6}Se_2$ and $K_xFe_2Se_2$. As mentioned before, $K_{0.8}Fe_{1.6}Se_2$ and $K_xFe_2Se_2$ are two phase-separated regions. If the same effective magnetic model describes both structures, it is very interesting to inquire into the magnetic configurations near the boundary of these two structures. We perform a Monte Carlo (MC) simulation on the J_1-J_2-J_3-K model[38] to address this problem. A simple numerical simulation, which includes a standard Markov chain MC simulation, followed by a zero-temperature relaxation process, is performed to qualitatively investigate the magnetic orders near the phase boundaries. A two-dimensional spin lattice $[L_x(L_{y1} + L_{y2})]$ is used with periodic boundary conditions (PBCs). Vacancies with the $\sqrt{5} \times \sqrt{5}$ pattern are created in L_{y1} regions for the $K_{0.8}Fe_{1.6}Se_2$ phase. A general result we obtained as shown in Fig. 4 is that the spin directions between the L_{y1} and L_{y2} regions are noncollinear. Since experimentally the ordered AFM moment is along the c axis in $K_{0.8}Fe_{1.6}Se_2$,[7] this result suggests that the ordered moment in the BAF state must be in the plane. This noncollinearity stems from the presence of vacancies and intrinsic magnetic frustration among the magnetic exchange couplings, similar to the study in the frustrated J_1-J_2 model.[43] Recent STM results have provided evidence supporting this prediction. It was shown that the magnetic moment induced by an individual vacancy in the SC state is indeed in the plane.[22]

The phase separation between the vacancy-ordered BAF state and the SC state has blurred the interplay between magnetism and superconductivity in alkali-doped iron selenide. The above results also clarify the connection. In iron pnictides, as increasing doping suppresses CAF order, superconductivity develops. The magnetic order is able to coexist with superconductivity in a small doping region.[44] Even in the region where the magnetic order is completely suppressed, orthorhombic lattice distortion which couples the fluctuating short-range CAF order[45,46] can survive and coexist with superconductivity. Our result suggests that similar physics can take place in $R_{1-x}Fe_{2-y}Se_2$. The absence of iron vacancies

in the SC state suggests that the true SC material has a chemical formula $R_{1-x}Fe_2Se_2$. The parent state of this material should be a BAF state. Increasing doping suppresses the BAF state and leads to SC. While it is still difficult to determine whether the BAF and SC can coexist, we can safely argue that, similar to iron pnictides, a lattice distortion as shown in Fig. 1(b) that couples to the short-range BAF fluctuation should be able to coexist with SC.

This picture provide explanations for many puzzling phenomena observed in alkali-doped iron selenides $R_{1-x}Fe_{2-y}Se_2$. First, in ARPES measurements, a weak but large electron pocket at the Γ point was observed.[6] This pocket is almost identical to the electron pockets at the M point, suggesting that the electron pocket is a folded pocket due to translational symmetry breaking in the SC state. Moreover, in a recent STM experiment,[21] a 2×2 charge density modulation with respect to the Fe lattice was observed to coexist with the SC phase. These electronic superstructures are consistent with the checkerboard phase. Second, neutron-scattering experiments suggested that the vacancy-ordered-AFM state interacts strongly with superconductivity.[8] In a phase-separation scenario, such a strong interaction is hard to understood. Our results resolve such a dilemma. The experiment can be easily understood because the BAF state strongly interacts with both the vacancy-ordered-AFM state and the SC state. The development of superconductivity is expected to strongly suppress the BAF state. Finally, the 2×2 ordering in insulating samples observed by transmission electron microscopy (TEM)[19,25] can be naturally interpreted as our checkerboard state with the BAF order. Previously it was interpreted as another vacancy-ordered phase.[19,25] Such an interpretation is unlikely because the TEM signal of this order is much weaker than that of the $\sqrt{5} \times \sqrt{5}$ vacancy order.

In summary, we show that alkali-doped iron selenides $R_{1-x}Fe_{2-y}Se_2$ have a checkerboard phase in which each of the four Fe sites group together in a tetragonal structure. The checkerboard phase approaches a BAF order in the absence of superconductivity. The phase also exhibits a $\sqrt{2} \times \sqrt{2}$ modulation charge ordering on Fe sites. Magnetic properties related to this state are calculated. Combining with the strong experimental evidence of phase separation between vacancy-ordered and vacancy-free phases, we suggest the checkerboard phase is the parent state of the superconductor.

We acknowledge helpful discussions with H. Ding, D. L. Feng, P. C. Dai, N. L. Wang, H. H. Wen, X. Chen, Q. K. Xue, T. Xiang, and Y. Y. Wang. W.L. gratefully acknowledges financial support by Fudan University. J.P. was supported by the 973 Projects of China (2012CB821400) and NSFC-11190024. S.D. was supported by the 973 Projects of China (2011CB922101), NSFC (11004027), and NCET (10-0325).

*jphu@iphy.ac.cn

[1] J. Guo, S. Jin, G. Wang, S. Wang, K. Zhu, T. Zhou, M. He, and X. Chen, Phy. Rev. B **82**, 180520(R) (2010).

[2] M.-H. Fang, H.-D. Wang, C.-H. Dong, Z.-J. Li, C.-M. Feng, J. Chen, and H. Q. Yuan, Europhys. Lett. **94**, 27009 (2011).

[3] R. H. Liu, X. G. Luo, M. Zhang, A. F. Wang, J. J. Ying, X. F. Wang, Y. J. Yan, Z. J. Xiang, P. Cheng, G. J. Ye, Z. Y. Li, and X. H. Chen, Europhys. Lett. **94**, 27008 (2011).

[4] Y. Zhang, L. X. Yang, M. Xu, Z. R. Ye, F. Chen, C. He, J. Jiang, B. P. Xie, J. J. Ying, X. F. Wang, X. H. Chen, J. P. Hu, and D. L. Feng, Nat. Mater. **10**, 273 (2011).

[5] X.-P. Wang, T. Qian, P. Richard, P. Zhang, J. Dong, H.-D. Wang, C.-H. Dong, M.-H. Fang, and H. Ding, Europhys. Lett. **93**, 57001 (2011).

[6] D. Mou *et al.*, Phys. Rev. Lett. **106**, 107001 (2011).

[7] W. Bao, Q. Huang, G. F. Chen, M. A. Green, D. M. Wang, J. B. He, X. Q. Wang, and Y. Qiu, Chin. Phys. Lett. **28**, 086104 (2011).

[8] W. Bao, G. N. Li, Q. Huang, G. F. Chen, J. B. He, M. A. Green, Y. Qiu, D. M. Wang, and J. L. Luo, e-print arXiv:1102.3674.

[9] M. Wang, C. Fang, D.-X. Yao, G. Tan, L. W. Harriger, Y. Song, T. Netherton, C. Zhang, M. Wang, M. B. Stone, W. Tian, J. Hu, and P. Dai, Nat. Commun. **2**, 580 (2011).

[10] C. Platt, R. Thomale, and W. Hanke, Ann. Phys. (Berlin) **523**, 638 (2011).

[11] S. Maiti, M. M. Korshunov, T. A. Maier, P. J. Hirschfeld, and A. V. Chubukov, Phys. Rev. Lett. **107**, 147002 (2011).

[12] Y.-Z. You, H. Yao, and D.-H. Lee, Phys. Rev. B **84**, 020406(R) (2011).

[13] T. A. Maier, S. Graser, P. J. Hirschfeld, and D. J. Scalapino, Phys. Rev. B **83**, 100515(R) (2011).

[14] C. Fang, Y.-L. Wu, R. Thomale, B. A. Bernevig, and J. Hu, Phys. Rev. X **1**, 011009 (2011).

[15] J. Hu and H. Ding, e-print arXiv:1107.1334.

[16] R. Yu, P. Goswami, Q. Si, P. Nikolic, and J.-X. Zhu, e-print arXiv:1103.3259.

[17] T. Saito, S. Onari, and H. Kontani, Phys. Rev. B **83**, 140512(R) (2011).

[18] C.-H. Li, B. Shen, F. Han, X. Zhu, and H.-H. Wen, Phys. Rev. B **83**, 184521 (2011).

[19] Y. J. Yan, M. Zhang, A. F. Wang, J. J. Ying, Z. Y. Li, W. Qin, X. G. Luo, J. Q. Li, J. Hu, and X. H. Chen, e-print arXiv:1104.4941.

[20] F. Chen, M. Xu, Q. Q. Ge, Y. Zhang, Z. R. Ye, L. X. Yang, J. Jiang, B. P. Xie, R. C. Che, M. Zhang, A. F. Wang, X. H. Chen, D. W. Shen, X. M. Xie, M. H. Jiang, J. P. Hu, and D. L. Feng, Phys. Rev. X **1**, 021020 (2011).

[21] P. Cai, C. Ye, W. Ruan, X. Zhou, A. Wang, M. Zhang, X. Chen, and Y. Wang, e-print arXiv:1108.2798.

[22] W. Li, H. Ding, P. Deng, K. Chang, C. Song, K. He, L. Wang, X. Ma, J.-P. Hu, X. Chen, and Q.-K. Xue, Nat. Phys. doi: 10.1038/NPHYS2155 (2011).

[23] R. H. Yuan, T. Dong, Y. J. Song, P. Zheng, G. F. Chen, J. P. Hu, J. Q. Li, and N. L. Wang, Sci. Rep. **2**, 221 (2012).

[24] A. M. Zhang, T. L. Xia, W. Tong, Z. R. Yang, and Q. M. Zhang, e-print arXiv:1203.1533.

[25] Z. Wang, Y. J. Song, H. L. Shi, Z. W. Wang, Z. Chen, H. F. Tian, G. F. Chen, J. G. Guo, H. X. Yang, and J. Q. Li, Phys. Rev. B **83**, 140505 (2011).

[26] J. Zhao, D. T. Adroja, D.-X. Yao, R. Bewley, S. Li, X. F. Wang, G. Wu, X. H. Chen, J. Hu, and P. Dai, Nat. Phys. **5**, 55 (2009).

[27] J. Zhao, D.-X. Yao, S. Li, T. Hong, Y. Chen, S. Chang, W. Ratcliff, J. W. Lynn, H. A. Mook, G. F. Chen, J. L. Luo, N. L. Wang, E. W. Carlson, J. Hu, and P. Dai, Phys. Rev. Lett. **101**, 167203 (2008).

[28] W. Bao, Y. Qiu, Q. Huang, M. A. Green, P. Zajdel, M. R. Fitzsimmons, M. Zhernenkov, S. Chang, M. Fang, B. Qian, E. K. Vehstedt, J. Yang, H. M. Pham, L. Spinu, and Z. Q. Mao, Phys. Rev. Lett. **102**, 247001 (2009).

[29] S. Li, C. de la Cruz, Q. Huang, Y. Chen, J. W. Lynn, J. Hu, Y.-L. Huang, F.-C. Hsu, K.-W. Yeh, M.-K. Wu, and P. Dai, Phys. Rev. B **79**, 054503 (2009).

[30] F. Ma, W. Ji, J. Hu, Z.-Y. Lu, and T. Xiang, Phys. Rev. Lett **102**, 177003 (2009).

[31] C. Fang, B. A. Bernevig, and J. Hu, Europhys. Lett. **86**, 67005 (2009).

[32] W.-G. Yin, C.-C. Lee, and W. Ku, Phys. Rev. Lett. **105**, 107004 (2010).

[33] W.-G. Yin, C.-H. Lin, and W. Ku, e-print arXiv:1106.0881.

[34] P. E. Blöchl, Phys. Rev. B **50**, 17953 (1994).

[35] G. Kresse and J. Furthmuller, Phys. Rev. B **54**, 11169 (1996).

[36] J. P. Perdew, K. Burke, and M. Ernzerhof, Phys. Rev. Lett. **77**, 3865 (1996).

[37] X.-W. Yan, M. Gao, Z.-Y. Lu, and T. Xiang, Phys. Rev. B **84**, 054502 (2011).

[38] J. Hu, B. Xu, W. Liu, N. Hao, and Y. Wang, e-print arXiv:1106.5169.

[39] C. Fang, B. Xu, P. Dai, T. Xiang, and J. Hu, e-print arXiv:1103.4599.

[40] A. L. Wysocki, K. D. Belashchenko, and V. P. Antropov, Nat. Phys.**7**, 485 (2011).

[41] F. Lu and X. Dai, e-print arXiv:1103.5521.

[42] R. Yu, P. Goswami, and Q. Si, Phys. Rev. B **84**, 094451 (2011).

[43] B. Xu, C. Fang, W. M. Liu, and J. Hu, e-print arXiv:1104.1848.

[44] D. C. Johnston, Adv. Phys. **59**, 803 (2010).

[45] C. Fang, H. Yao, W.-F. Tsai, J. P. Hu, and S. A. Kivelson, Phys. Rev. B **77**, 224509 (2008).

[46] C. Xu, M. Müller, and S. Sachdev, Phys. Rev. B **78**, 020501(R) (2008).